Evidence for Vacancy-Related Recombination Active Defects in as-Grown N-Type Czochralski Silicon

P. Zheng, F. E. Rougieux, N. E. Grant, and D. Macdonald

***Abstract*—A recombination of active defect in very high lifetime Czochralski grown *n*-type silicon wafers, which can be thermally deactivated at 150 °C, is described. In addition, the existence of a recently measured defect, which is deactivated at 350 °C, is confirmed. Both defects are found to significantly degrade the lifetime of millisecond-range Czochralski-grown *n*-type silicon wafers: a material widely used for high-efficiency solar cells. The observed deactivation temperature suggests that it may be caused by vacancy-phosphorus pairs. The deactivation temperature of the second defect is consistent with the presence of vacancy-oxygen (V-O) pairs.**

***Index Terms*—As-grown, Czochralski (Cz), defects, silicon.**

I. Introduction

FOR decades, *p*-type silicon has been the dominant material for solar cells. However, within the past several years, metallic-related impurities, such as iron and the boron–oxygen defect, have been found to significantly degrade the performance of p-type silicon solar cells. By contrast, the same defects in n-type silicon have been shown to have little impact on its electronic quality [1]–[7]. However, other defects related to the presence of silicon vacancies, self-interstitials, and complexes formed with dopant atoms or light elements, such as oxygen, carbon, and nitrogen, are more likely to limit the performance of n-type solar cells. In particular, Czochralski (Cz) silicon ingots grown for photovoltaics are generally pulled relatively rapidly, leading to vacancy-rich conditions along many of the ingots. It is, therefore, plausible that vacancy-related centers could play a role in terms of recombination in these materials. However, to date, there have been few studies on these types of defects in terms of their impact on carrier lifetimes.

The thermal stability and the energy level of vacancy or interstitial related defects in silicon have been extensively studied and are well known from deep-level transient spectroscopy (DLTS) [8]–[10], electron paramagnetic resonance (EPR), positron annihilation, and localized vibrational mode spectroscopy [11]–[13]. The defects in these studies were intentionally created using electron and proton irradiation, leading to much higher concentrations of defects than generally occurred in as-grown silicon wafers. In any case, the impact of such intrinsic point defects on the minority-carrier lifetime remains unclear.

A recent study from Rougieux *et al*. [14] has demonstrated that a lifetime-limiting defect in the as-grown state of Cz n-type silicon can be thermally deactivated between 300 and 350 °C. It was suggested that the defect was related to intrinsic point defects, possibly vacancy-oxygen (V-O) pairs.

In this paper, we further investigate the thermal stability of grown-in point defects in the as-grown state of high lifetime Cz n-type silicon wafers using minority-carrier lifetime measurements. In addition to the defect observed by Rougieux *et al*., we also observe a second defect, which is thermally deactivated at even lower temperatures. We have determined the deactivation temperature range and annihilation activation energy of this second lower temperature defect.

II. Experimental Methods

The samples used in this study were three *n*-type Cz grown monocrystalline phosphorous-doped silicon wafers. All wafers had a diameter of 4 in and thickness of 1 μm and were not subject to any thermal treatment after being sawn from the ingot. Two wafers had a resistivity of 0.4 $\Omega \cdot$cm, and one wafer had a resistivity of 0.75 $\Omega \cdot$cm. All wafers were diced into quarters. The study of the annihilation mechanism of the defects was performed at temperatures between 100 and 450 °C. For temperatures below 250 °C, wafers were annealed in a conventional oven in air. For temperatures higher than 250 °C, the samples were annealed in a quartz tube furnace in nitrogen ambient. The annealing was followed by rapid cooling in air.

The thermal stability of grown-in defects was then investigated using minority-carrier lifetime measurements with a room-temperature surface-passivation technique [15]. In this technique, silicon wafers were prepared by etching the samples for 10 min in 25 wt% tetramethylammonium hydroxide (TMAH) at 60–70 °C and, subsequently, cleaned using RCA1 at ~70 °C for 10 min. This etch and clean procedure was performed before each passivation round in order to remove surface defects and to ensure a low surface recombination velocity (S). Following the TMAH etch and RCA 1 clean, the silicon wafers were then immersed in a plastic container filled with 150 mL of 20 wt% HF and subsequently illuminated to activate the passivation, as described by Grant *et al*. [15]. The method allows bulk lifetimes well above 1 ms to be reliably measured. Immediately after illumination, the samples were measured by a transient photoconductance decay method using a WCT-120 Sinton lifetime tester. To account for any variations in surface recombination after each chemical treatment step, an n-type float zone (FZ) monocrystalline silicon wafer of

Manuscript received August 28, 2014; revised October 17, 2014; accepted October 28, 2014. This work was supported by the Australian Research Council Future Fellowships program and the Australian Renewable Energy Agency Fellowships program.

The authors are with the Research School of Engineering, College of Engineering and Computer Science, The Australian National University, Canberra ACT 0200, Australia (e-mail: peiting.zheng@anu.edu.au; fiacre.rougieux@anu.edu.au; nicholas.grant@anu.edu.au; daniel.macdonald@anu.edu.au).

Color versions of one or more of the figures in this paper are available online at http://ieeexplore.ieee.org.

Digital Object Identifier 10.1109/JPHOTOV.2014.2366687

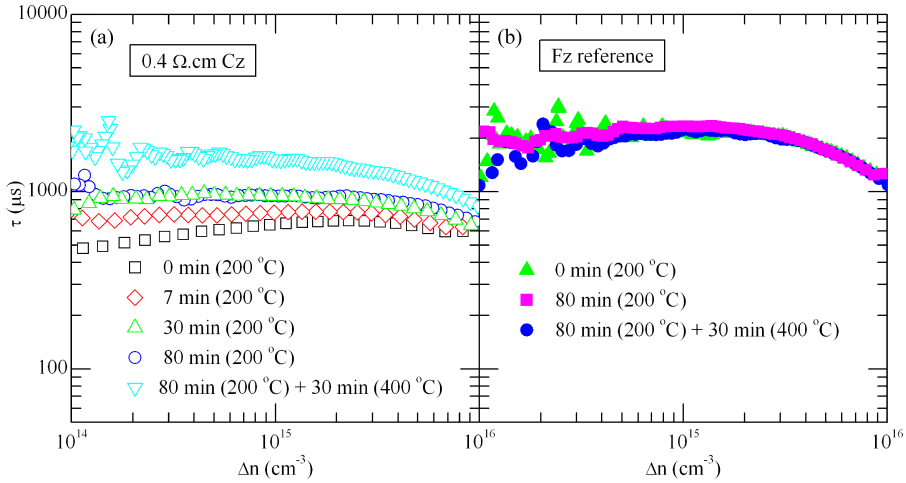

Fig. 1. Injection dependence of the measured lifetime for (a) 0.4 Ω · cm Cz samples annealed at 200 °C for different lengths of time (total of 80 min), followed by a 400 °C annealing furnace for 30 min. (b) FZ control wafer annealed at 200 °C for a total of 80 min, followed by a 400 °C annealing for 30 min.

resistivity 1.5 Ω · cm was used as a control. The same samples were reused for subsequent anneals at a given temperature. Each time, approximately 10 μm of silicon was removed by etching prior to each HF passivation.

III. Results and Discussion

A. Temperature-Dependent Defect Deactivation

Fig. 1(a) plots the injection dependence of the effective minority-carrier lifetime, where the hollow symbols correspond to the 0.4 Ω · cm samples annealed at 200 °C for 0, 7, 30, and 80 min. Following the 200 °C anneal, the samples were annealed at 400 °C for 30 min. The graph shows an increase of lifetime from 600 μs (at $\Delta n = 0.1 \times n_0$) in the as-grown state, to 850 μs after 7 min annealing. The lifetime increases to 1 ms after a further 23 min (30 min in total) annealing and remains at 1 ms after a total of 80 min, indicating longer annealing times would not further improve the lifetime. However, when the samples were subject to a 400 °C anneal for 30 min, τ_{eff} improves again from 1 to 1.5 ms.

To ascertain whether the improvements in τ_{eff} were due to a reduction in bulk or surface recombination, the FZ control wafer underwent the same annealing sequence as the Cz samples. Contrary to the Cz samples, the lifetime of the FZ control remained stable, as represented by the solid symbols in Fig. 1(b).

The lifetime of the 0.75 Ω · cm sample behaved similarl to the 0.4 Ω · cm sample, where the lifetime improved from 2.1 to 2.6 ms after 30 min annealing at 185 °C and did not show significant change over a total of 3 h annealing at 185 °C. The lifetime was then found to increase further to 3.4 ms after a 450 °C anneal for 30 min. The lifetime data for the 0.75 Ω · cm material is shown in Fig. 2. From these observations, it is found that the defects are recombination active and undergo a two-stage annihilation mechanism. In addition, the temperature range of the first stage defect is similar to the well-known boron–oxygen defect [5], [16]. However, it is important to note that the only dopant species in the samples is phosphorus (no boron); hence,

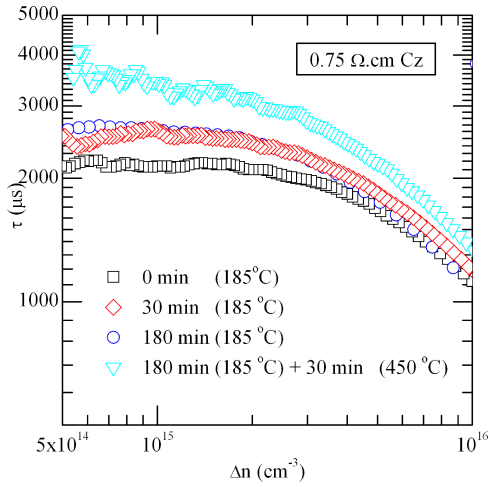

Fig. 2. Injection dependence of the measured lifetime for 0.75 Ω · cm Cz samples annealed at 185 °C for a total of 180 min, followed by a 450 °C annealing for 30 min.

the observed defect is not related to the boron–oxygen defect. In addition, we do not observe any lifetime degradation after 24 h illumination for these samples when passivated by a-Si:H, providing further evidence that the defect is not the boron–oxygen defect.

In order to investigate the two-stage defect annihilation mechanism, we have determined the threshold temperature, at which the defect annihilation begins and the temperature at which it is complete. The samples were annealed for a fixed time of 30 min at different temperatures ranging from 100 to 450 °C. To determine the change of defect concentration in the samples, the normalized effective defect density is calculated by [14]

$$\frac{N^*_{t.\text{anneal}}}{N^*_{t.0}} = \frac{\dfrac{1}{\tau_{\text{eff}-\text{anneal}}} - \dfrac{1}{\tau_{\text{eff}\,\infty}}}{\dfrac{1}{\tau_{\text{eff}\,0}} - \dfrac{1}{\tau_{\text{eff}\,\infty}}} \tag{1}$$

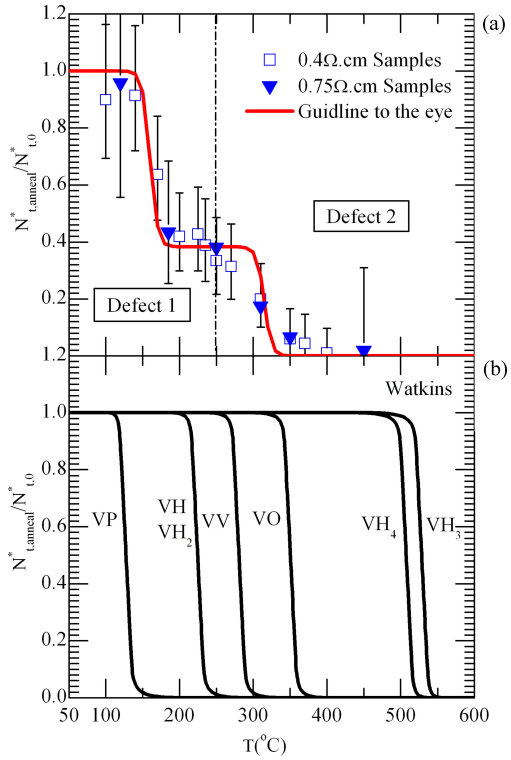

Fig. 3. Normalized effective defect density for (a) 0.4 Ω · cm wafers and 0.75 Ω · cm wafers after 30 min annealing over a temperature range of 100 to 450 °C. The line is there to guide the eye. (b) 30 min isochronal anneal for temperatures ranging from 0 to 600 °C measured by EPR from Watkins [11].

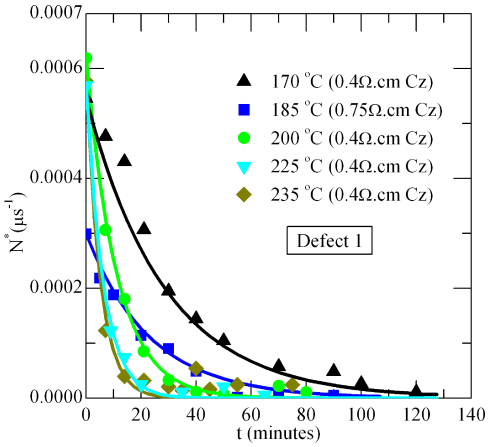

Fig. 4. Effective defect concentration (N^*) versus annealing time, where the wafer used for 185 °C is 0.75 Ω · cm, and the others are 0.4 Ω · cm wafers. The lines are fitting to the data using (3).

where $\tau_{\text{eff}0}$ is the measured effective lifetime in the as-grown state, $\tau_{\text{eff}-\text{anneal}}$ is the annealed effective lifetime at any given temperature after 30 min annealing, and $\tau_{\text{eff}\,\infty}$ is the maximum lifetime where all metastable defects are suppressed. For practical purposes, we obtain $\tau_{\text{eff}\,\infty}$ by taking the average value of effective lifetime data of the wafers after an anneal of at least 2 h at 400 and 450 °C to ensure that the effective lifetime has reached a stable value. In this paper, the normalized effective defect concentration was determined at an injection level of 10% of the net doping $\Delta n = 0.1 \times n_0$.

Fig. 3(a) shows the remaining defect density after isochronal annealing of 30 min for temperatures ranging from 100 to 450 °C. Data for both resistivities of 0.4 and 0.75 Ω · cm are shown. The uncertainty of the normalized effective defect density is estimated by assuming a ±5% uncertainty in the measurement of carrier lifetime [17]. The graph shows two annealing stages, as previously indicated in Figs. 1(a) and 2. For the first annealing stage, the normalized effective defect concentration remains flat below 150 °C, and starts to decrease sharply between 150 and 200 °C. The normalized effective defect concentration stabilizes between 200 and 300 °C and starts to decrease again beyond that. For a 30 min anneal, the second annealing stage occurs between 300 and 350 °C. The defect concentration then remains stable up to 450 °C. The two annealing stages could involve two forms of the same defect, or two entirely different species of defect. This will be discussed in more detail in the next section.

Similar results for the remaining defect density after isochronal annealing have been presented previously by Watkins [11] using EPR shown in Fig. 3(b). The lower temperature defect in our samples is deactivated over a temperature range of 150 to 200 °C, similar to the vacancy-phosphorous (V-P) pairs, as observed by Watkins. The higher temperature defect we observe is deactivated over temperatures ranging between 300 and 350 °C, a similar range to the defect recently observed by Rougieux *et al*. In comparison with Watkins's data, this result lies closest to the V-O pairs.

The defect observed by Rougieux *et al*. [14] using the same minority-carrier lifetime and passivation techniques was observed in n-type Cz wafers of lower phosphorus concentration, with deactivation occurring over a temperature range of 300 to 350 °C. However, in that study, no change of lifetime was observed in the lower temperature range that corresponds to the lower temperature defect reported in this paper. A possible reason for this is that the phosphorous concentration in the samples from the earlier study is approximately an order of magnitude less than in the samples used in this study. The fact that the samples with higher doping have higher effective defect densities supports the hypothesis that the lower temperature defect is caused by V-P pairs.

B. Activation Energy for Annihilation of the First-Stage Defect

An alternative possible way to identify the defect is through its characteristic annihilation energy. Thus, we have determined the annihilation activation energy E_{ann} for the lower temperature defect, and compare it with the E_{ann} values from the literature for known defects.

By monitoring τ_{eff} versus the annealing time t, the effective defect concentration N^* can be extracted from [16]

$$N^*(t,T) = \frac{1}{\tau_{\text{eff}}(t)} - \frac{1}{\tau_{\text{eff}\,\infty}} \tag{2}$$

where $\tau_{\text{eff}}(t)$ is the effective lifetime of the sample after t minutes annealing at any given temperature. Fig. 4 shows the

isothermal evolution of τ_{eff} for five different temperatures ranging from 170 to 235 °C. Note that the wafer used for the annealing at 185 °C has a resistivity of 0.75 $\Omega \cdot$ cm, while the remaining wafers have a resistivity of 0.4 $\Omega \cdot$ cm, hence the lower starting defect concentration. The normalized effective defect concentration N^* follows an exponential decay during the annihilation process

$$N^*(t,T) = N_0^*[\exp(-R_{\text{ann}}(T)t] \tag{3}$$

where N_0^* corresponds to the value of N^*at $t = 0$, where the wafers are in the as-grown state. Thus, by fitting the isothermal experimental N^*data with (3), the annihilation rate $R_{\text{ann}}(T)$ at each temperature can be determined. As the annihilation mechanism of the defect is thermally activated, the annihilation activation energy E_{ann} can then be obtained from an Arrhenius plot of the variation of R_{ann} with temperature according to the following expression [18], where k_0 is a scaling constant and k_B is Boltzmann's constant

$$R_{\text{ann}}(T) = k_0 \exp\left(-\frac{E_{\text{ann}}}{k_B T}\right). \tag{4}$$

From Fig. 4, we can see a clear exponential decay trend of the normalized defect concentration at five different temperatures. At 185 °C, the exponential decay starts with a lower normalized defect concentration than others. For this temperature, a wafer of higher resistivity was used; however, the resistivity does not appear to have an impact on the annihilation rate. From these results, we then evaluate the R_{ann} at each temperature. To determine R_{ann}, we take the logarithm of both sides of (3). We then obtain a linearized equation of the form

$$\ln[N^*(t,T)] = -R_{\text{ann}}(T)t + \ln(N_0^*). \tag{5}$$

As shown in (5), we can determine R_{ann} by taking the slope of the linearized relationship using a least squares fit. However, if we use the data of N^*close to 0, a large error in $\ln(N^*)$ results, and the slope of the linear regression is affected significantly. Therefore, in the following calculations, data which has reached $\pm 5\%$ of the maximum value of the lifetime is ignored in the calculation. The uncertainty of the activation energy is estimated by assuming a $\pm 5\%$ uncertainty in the measurement of carrier lifetime. Fig. 5 shows the least squares fit for the data from Fig. 4. The linear regression fits well with the data and results in a good correlation of 0.98–0.993. Note that the large error bars for some of the data results from the value of N^*approaching zero.

Using the $R_{\text{ann}}(T)$ computed using (3) and (5), the variation of R_{ann} with T is plotted in Fig. 6. R_{ann} is found to follow the Arrhenius law. We use a statistical method to calculate the prediction interval for $\ln(N^*)$, and estimate a confidence interval from the slope of the linear regression; thus, we can estimate the error in E_{ann}. It gives a value of 0.57 ± 0.16 eV. However, the accuracy of the statistical method may be somewhat limited by the relatively small datasets in some cases and may, therefore, somewhat underestimate the final uncertainty.

The annihilation activation energy calculated using a more conservative error tracing method is 0.64 ± 0.44 eV. In this case, the large uncertainty in E_{ann} results from the amplification of the error in N^* after taking the logarithm. It can be considered as yielding a conservative upper and lower bounds for E_{ann}.

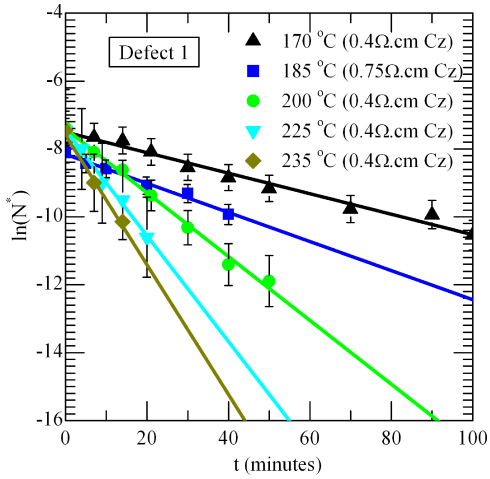

Fig. 5. Least squares fits for $\ln(N^*)$ as a function of annealing time using (5) for different temperatures. The lines are fitting to data using (5).

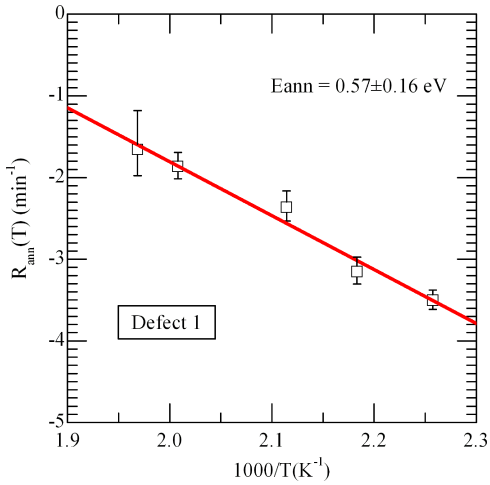

Fig. 6. Arrhenius plot with least squares fit for $R_{\text{ann}}(T)$ as a function of temperature using (4).

Various studies have reported the annealing behavior of V-P pairs around 150 °C. Hirata *et al.* [19] and Kimerling *et al.* [20] created V-P pairs by irradiating lightly doped FZ n-type wafers using a Co^{60} gamma-ray source at room temperature; thus, allowing them to investigate the annealing characteristics of the V-P defect. Dannefaer *et al.* [12] utilized the same approach to create vacancies; however, they used n-type Cz wafers with an oxygen concentration of 1×10^{18} cm^{-3}. The activation energy values from the literature are summarized in Table I.

It has also been previously shown that the annihilation activation energy of V-P pairs depends on the charge state. In order to compare the activation energy calculated in this study, we have to determine the charge state of V-P pairs. The charge state of the V-P pair depends on the Fermi level of the wafer and, thus, the doping density in the wafer and the energy level of the defect in the bandgap. Various studies have shown that

TABLE I
ACTIVATION ENERGY VALUES FROM THE LITERATURE FOR ANNIHILATION OF INTRINSIC-DEFECT RELATED COMPLEXES IN SILICON

Authors	Activation Energy (E_{ann}) eV	Characterization Method	Type of Defects	Phosphorus Doping Concentration (cm^{-3})
Hirata *et al*.	0.93 ± 0.05	Lifetime measurement	V-P^0	1×10^{14}
Kimerling *et al*.	0.95 ± 0.05	Junction capacitance transient technique	V-P^0	5×10^{15}
Kimerling *et al*.	1.25 ± 0.05	Junction capacitance transient technique	V-P^-	5×10^{15}
Dannefaer *et al*.	0.8 ± 0.2 eV	Positron annihilation	V-P^0	5×10^{15} to 5×10^{18}
This Study	0.57 ± 0.16 eV	Lifetime measurement	—	6.6×10^{15} to 1.3×10^{16}

V-P pairs have an acceptor level in the bandgap at EC –0.4 eV determined by Hall effect measurements [21]–[23] (EC is the conduction bandedge). The V-P pairs are negatively charged, while the Fermi level is above the defect energy level and neutral, otherwise, as suggested by Kimerling *et al*. and Watkins [11], [20]. In this study, the doping density of the samples is approximately 6.6×10^{15} to 1.3×10^{16} cm^{-3}. The V-P pairs in these samples are negatively charged at room temperature; however, in the temperature range of 150–200 °C, the Fermi level shifts down to a value below or similar to the defect energy level (about EC -0.44 eV for 200 °C and EC -0.39 eV for 150 °C). Therefore, the V-P pairs are neutral during annealing. We compare our E_{ann} result with V-P^0 in Table I. Our result lies in or close to the range of activation energy values reported above and best matches with Dannefaer's data (with similar sample conditions to ours). Dannefaer *et al*. also reported a second annealing stage and suggested that the annealing is associated with the phosphorus-vacancy-oxygen complex, which is stable at 250 °C for at least 250 h but unstable at 300 °C or above. Therefore, the defect found in the second annealing stage in this study may involve both phosphorus and vacancies and not simply V-O pairs.

A possible scenario has been suggested by Rougieux *et al*. regarding the formation of recombination active defects during ingot growth. Rougieux *et al*. suggested that during ingot cool down, free vacancies pair with oxygen around 360 °C, other vacancies at around 270 °C, and potentially phosphorus near 140 °C. In that case, the lifetime was limited by what appears to be the V-O defect. In such a scenario, the V-O defect would correspond to defect 2 observed here, while defect 1 would be V-P pairs. Note that, in general, comparison between ingots and even within one ingot is not straightforward, as the vacancy concentration could potentially be significantly different [24].

Finally, we note that DLTS measurements are unlikely to detect the defects studied here, due to their very low concentrations. Based on the typical values of carrier capture cross sections of 10^{-14} cm^2 and the lifetimes measured with full defect activation, we estimate that the defect concentrations are below 10^{10} cm^{-3}, which is below the sensitivity limit of conventional DLTS systems for wafers of the resistivities used here.

IV. CONCLUSION

In summary, we have studied a lifetime limiting grown-in defect in high-lifetime n-type Cz-grown silicon wafers. We also confirm the existence of another recently measured recombination active defect in n-type Cz grown silicon wafers. The defects can be thermally deactivated in two different annealing stages. The first stage occurs between 150 and 200 °C and the second stage between 300 and 350 °C. We observe a threefold increase in the lifetime from 0.5 to 1.5 ms for the 0.45 $\Omega \cdot$ cm samples and from 2 to 3.4 ms for the 0.75 $\Omega \cdot$ cm sample at an injection level of $\Delta n = 0.1 \times n_0$. The annihilation activation energy measured for the first stage defect is estimated to be 0.57 ± 0.16 eV. A potential candidate for the first stage defect could be V-P pairs, which are known to anneal out in the temperature range observed by Watkins [11]. V-O pairs are a possible candidate for the second-stage defect investigated in this study. The suggestion that V-P pairs are responsible for the first defect is also supported by the heavier doping in the samples studied here, in comparison with the previous study in which they were not observed. However, the relatively weak agreement between measured annihilation activation energy and the values from literature indicates that the identification of the first-stage defect is speculative and other defect (maybe not seen in previous studies) could also be responsible. Together with a previous study, our results indicate that grown-in vacancy-related point defects formed during ingot growth can significantly affect the bulk lifetime of high-quality n-type silicon wafers. The mitigation of these defects during solar cell processing will improve the solar cell efficiency, especially for solar cells processed at low temperature such as heterojunction solar cells. An improved awareness of the presence and properties of these low-temperature defects should also allow better correlation between lifetimes measured in the as-grown state, as well as final device performance.

REFERENCES

[1] K. Bothe, J. Schmidt, and R. Hezel, "Effective reduction of the metastable defect concentration in boron-doped czochralski silicon for solar cells," in *Proc. 29th IEEE Photovoltaic Spec. Conf.*, 2002, pp. 194–197.

[2] J. E. Cotter, J. H. Guo, P. J. Cousins, M. D. Abbott, F. W. Chen, and K. C. Fisher, "P-type versus n-type silicon wafers: prospects for high-efficiency commercial silicon solar cells," *IEEE Trans. Electron Devices*, vol. 53, no. 8, pp. 1893–1901, Aug. 2006.

[3] D. Macdonald and L. J. Geerligs, "Recombination activity of interstitial iron and other transition metal point defects in p- and n-type crystalline silicon," *Appl. Phys. Lett.*, vol. 85, pp. 4061–4063, 2004.

[4] S. Martinuzzi, O. Palais, M. Pasquinelli, D. Barakel, and F. Ferrazza, "N-type multicrystalline silicon wafers for solar cells," in *Proc. 31st IEEE Photovoltaic Spec. Conf.*, 2005, pp. 919–922.

[5] J. Schmidt and K. Bothe, "Structure and transformation of the metastable boron- and oxygen-related defect center in crystalline silicon," *Phys. Rev. B*, vol. 69, pp. 024107-1–024107-7, 2004.

[6] J. Broisch, J. Schmidt, J. Haunschild, and S. Rein, "UMG n-type Cz-silicon: Influencing factors of the light-induced degradation and its suitability for PV production," *Energy Procedia*, vol. 55, pp. 526–532, 2014.

[7] B. Lim, F. Rougieux, D. Macdonald, K. Bothe, and J. Schmidt, "Generation and annihilation of boron–oxygen-related recombination centers in compensated p- and n-type silicon," *J. Appl. Phys.*, vol. 108, pp. 103722-1–103722-9, 2010.

[8] J. H. Evans-Freeman, A. R. Peaker, I. D. Hawkins, P. Y. Y. Kan, J. Terry, L. Rubaldo, M. Ahmed, S. Watts, and L. Dobaczewski, "High-resolution DLTS studies of vacancy-related defects in irradiated and in ion-implanted n-type silicon," *Mater. Sci. Semicond. Process.*, vol. 3, pp. 237–241, 2000.

[9] F. D. Auret and P. N. K. Deenapanray, "Deep level transient spectroscopy of defects in high-energy light-particle irradiated si," *Crit. Rev. Solid State Mater. Sci.*, vol. 29, pp. 1–44, 2004.

[10] A. Chantre and L. C. Kimerling, "Configurationally multistable defect in silicon," *Appl. Phys. Lett.*, vol. 48, pp. 1000–1002, 1986.

[11] G. D. Watkins, "Intrinsic defects in silicon," *Mater. Sci. Semicond. Process.*, vol. 3, pp. 227–235, 2000.

[12] S. Dannefaer, G. Suppes, and V. Avalos, "Evidence for a vacancy–phosphorus–oxygen complex in silicon," *J. Phys., Condens. Matter*, vol. 21, pp. 015802-1–015802-6, 2009.

[13] J. Makinen, P. Hautojarvi, and C. Corbel, "Positron annihilation and the charge states of the phosphorus-vacancy pair in silicon," *J. Phys., Condens. Matter*, vol. 4, pp. 5137–5154, 1992.

[14] F. E. Rougieux, N. E. Grant, and D. Macdonald, "Thermal deactivation of lifetime-limiting grown-in point defects in n-type Czochralski silicon wafers," *Physica Status Solidi—Rapid Res. Lett.*, vol. 7, pp. 616–618, 2013.

[15] N. E. Grant, K. R. McIntosh, and J. T. Tan, "Evaluation of the bulk lifetime of silicon wafers by immersion in hydrofluoric acid and illumination," *ECS J. Solid State Sci. Technol.*, vol. 1, pp. 55–61, Jan. 1, 2012.

[16] J. Schmidt, K. Bothe, and R. Hezel, "Formation and annihilation of the metastable defect in boron-doped Czochralski silicon," in *Proc. IEEE 29th Photovoltaic Spec. Conf.*, 2002, pp. 178–181.

[17] J. Tan, D. Macdonald, F. Rougieux, and A. Cuevas, "Accurate measurement of the formation rate of iron–boron pairs in silicon," *Semicond. Sci. Technol.*, vol. 26, pp. 055019-1–055019-5, 2011.

[18] T. Schutz-Kuchly, J. Veirman, S. Dubois, and D. R. Heslinga, "Light-induced-degradation effects in boron–phosphorus compensated n-type czochralski silicon," *Appl. Phys. Lett.*, vol. 96, pp. 093505-1–093505-3, 2010.

[19] M. Hirata, M. Hirata, and H. Saito, "The interactions of point defects with impurities in silicon," *J. Phys. Soc. Jpn.*, vol. 27, pp. 405–414, 1969.

[20] L. C. Kimerling, H. M. DeAngelis, and J. W. Diebold, "On the role of defect charge state in the stability of point defects in silicon," *Solid State Commun.*, vol. 16, pp. 171–174, 1975.

[21] G. D. Watkins and J. W. Corbett, "Defects in irradiated silicon: Electron paramagnetic resonance and electron-nuclear double resonance of the Si-e center," *Phys. Rev.*, vol. 134, pp. A1359–A1377, 1964.

[22] H. Saito and M. Hirata, "Nature of radiation defects in silicon single crystals," *Jpn. J. Appl. Phys.*, vol. 2, pp. 678–687, 1963.

[23] M. Hirata, M. Hirata, H. Saito, and J. H. Crawford, "Effect of impurities on the annealing behavior of irradiated silicon," *J. Appl. Phys.*, vol. 38, pp. 2433–2438, 1967.

[24] V. V. Voronkov and R. Falster, "Grown-in microdefects, residual vacancies and oxygen precipitation bands in czochralski silicon," *J. Crystal Growth*, vol. 204, pp. 462–474, 1999.

Authors' photographs and biographies not available at the time of publication.